REPORT

VALLEYTRONICS

Large, valley-exclusive Bloch-Siegert shift in monolayer WS_2

Edbert J. Sie,[1] Chun Hung Lui,[2] Yi-Hsien Lee,[3] Liang Fu,[1] Jing Kong,[4] Nuh Gedik[1]*

Coherent interaction with off-resonance light can be used to shift the energy levels of atoms, molecules, and solids. The dominant effect is the optical Stark shift, but there is an additional contribution from the so-called Bloch-Siegert shift that has eluded direct and exclusive observation in solids. We observed an exceptionally large Bloch-Siegert shift in monolayer tungsten disulfide (WS_2) under infrared optical driving. By controlling the light helicity, we could confine the Bloch-Siegert shift to occur only at one valley, and the optical Stark shift at the other valley, because the two effects obey opposite selection rules at different valleys. Such a large and valley-exclusive Bloch-Siegert shift allows for enhanced control over the valleytronic properties of two-dimensional materials.

The fundamental interaction between light and matter can be understood within the framework of a two-level system with an energy splitting E_0 (*1*, *2*). Driving the system by off-resonance light of frequency $\hbar\omega < E_0$ produces a series of photon-dressed states (Floquet states) that are evenly spaced by $\hbar\omega$, where $\hbar$ is Planck's constant divided by 2π. In the first order, there are two pairs of photon-dressed states, one pair between the two original states (Fig. 1A) and the other pair outside the original states (Fig. 1B). Interactions between the original states and these photon-dressed states can be understood in terms of state repulsion. The former case leads to a shift of transition energy called the optical Stark shift, which increases linearly with the light intensity ($\mathcal{E}_0^2$) and inversely with the detuning energy, $\Delta E_{OS} \propto \mathcal{E}_0^2/(E_0 - \hbar\omega)$ (*3*). The latter case also leads to a shift called the Bloch-Siegert shift, which has a different energy dependence, $\Delta E_{BS} \propto \mathcal{E}_0^2/(E_0 + \hbar\omega)$ (*4*). Although the Bloch-Siegert shift is negligible at small detuning, at large detuning it can become comparable to the optical Stark shift.

The Bloch-Siegert shift has played an important role in atomic physics, notably for its manifestation as the Lamb shift in quantum electrodynamics (*5*, *6*) and its contribution to the trapping potential for cold atoms (*7*). In condensed matter physics, however, the Bloch-Siegert shift is a very rare finding because of its typically small magnitude (<1 μeV); so far it has been revealed only indirectly in artificial atoms by subtracting the dominant optical Stark shift using sophisticated modeling (*8*–*10*). To elucidate the detailed characteristics of the Bloch-Siegert shift, it is necessary to separate the two effects. Given that they are time-reversed partners of each other—the optical Stark shift arises from the corotating field and the Bloch-Siegert shift from the counterrotating field—it is theoretically possible to separate them under stimulation that breaks time-reversal symmetry.

We report the observation of a large Bloch-Siegert shift (ΔE_{BS} ~ 10 meV) that can be entirely separated from the optical Stark shift. Such a large and exclusive Bloch-Siegert shift is realized in a monolayer of the transition-metal dichalcogenide (TMD) WS_2. This is possible because this material system possesses two distinctive features. First, it exhibits strong light-exciton interaction at the two time-reversed valleys (K and K') in the Brillouin zone (Fig. 2, A to C) (*11*–*13*). Second, the two valleys possess finite and opposite Berry curvature because of the lack of inversion symmetry, giving rise to distinct optical selection rules and related valleytronic properties (*14*–*22*). That is, the optical transitions at the K and K' valleys are coupled exclusively to left-handed (σ^-) and right-handed (σ^+) circularly polarized light, respectively. Such a unique material platform allows us to separate the Bloch-Siegert shift from the optical Stark shift by using circularly polarized light.

Our experimental setup uses femtosecond pump-probe absorption spectroscopy (Fig. 2A). All measurements are carried out at room temperature. After pumping a monolayer of WS_2 with intense σ^- infrared light pulses, we probe the energy shift at the K valley with σ^- visible light pulses and that at the K' valley with σ^+ visible light pulses. A blueshift of the exciton absorption peak (α) is manifested as a differential curve in the absorption change Δα (Fig. 2C). From this, we can deduce the magnitude of the energy shift at both valleys. Previously, transient absorption with visible pumping has been used to study the optical Stark effect in monolayer TMDs (*23*, *24*). Here, by pumping with infrared light, we reveal the Bloch-Siegert shift in WS_2.

Shown in Fig. 2, D to G, are our results at the K valley (blue curve) and K' valley (red curve). For comparison, we first show the Δα spectra under zero-delay pumping at $\hbar\omega$ = 1.82 eV (Fig. 2D). For this small detuning energy, only the K valley shows an appreciable Δα signal. This signal arises from the optical Stark shift, which occurs exclusively at

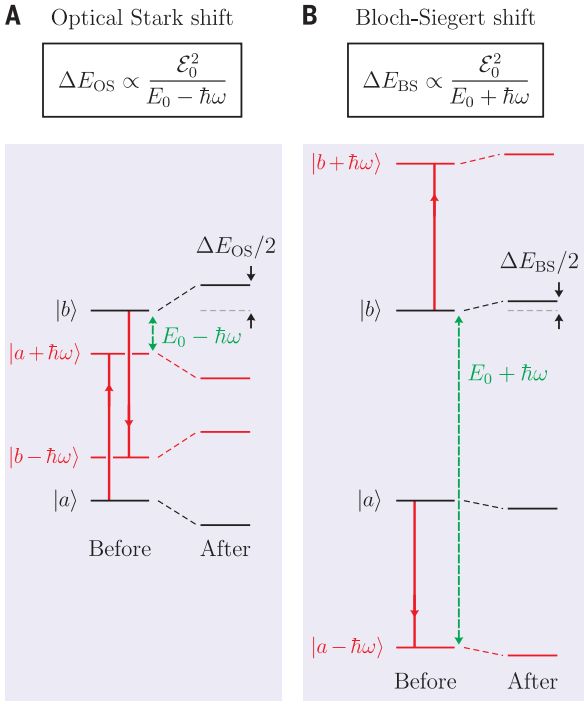

Fig. 1. Comparison of the optical Stark shift and the Bloch-Siegert shift in a two-level system. (**A**) Energy diagram for optical Stark shift. $|a\rangle$ and $|b\rangle$ denote the two original states with resonance energy E_0 before they are optically driven; $|a + \hbar\omega\rangle$ and $|b - \hbar\omega\rangle$ are photon-dressed (Floquet) states driven by the corotating optical field. Hybridization with these Floquet states causes the resonance energy to blueshift by ΔE_{OS}, which is proportional to the light intensity ($\mathcal{E}_0^2$) and inversely proportional to $(E_0 - \hbar\omega)$. (**B**) Energy diagram for Bloch-Siegert shift. $|a - \hbar\omega\rangle$ and $|b + \hbar\omega\rangle$ are two different Floquet states driven by the counterrotating optical field. Hybridization with these Floquet states causes the Bloch-Siegert shift, with magnitude ΔE_{BS} inversely proportional to $(E_0 + \hbar\omega)$.

[1]Department of Physics, Massachusetts Institute of Technology, Cambridge, MA 02139, USA. [2]Department of Physics and Astronomy, University of California, Riverside, CA 92521, USA. [3]Materials Science and Engineering, National Tsing-Hua University, Hsinchu 30013, Taiwan. [4]Department of Electrical Engineering and Computer Science, Massachusetts Institute of Technology, Cambridge, MA 02139, USA.
*Corresponding author. Email: gedik@mit.edu

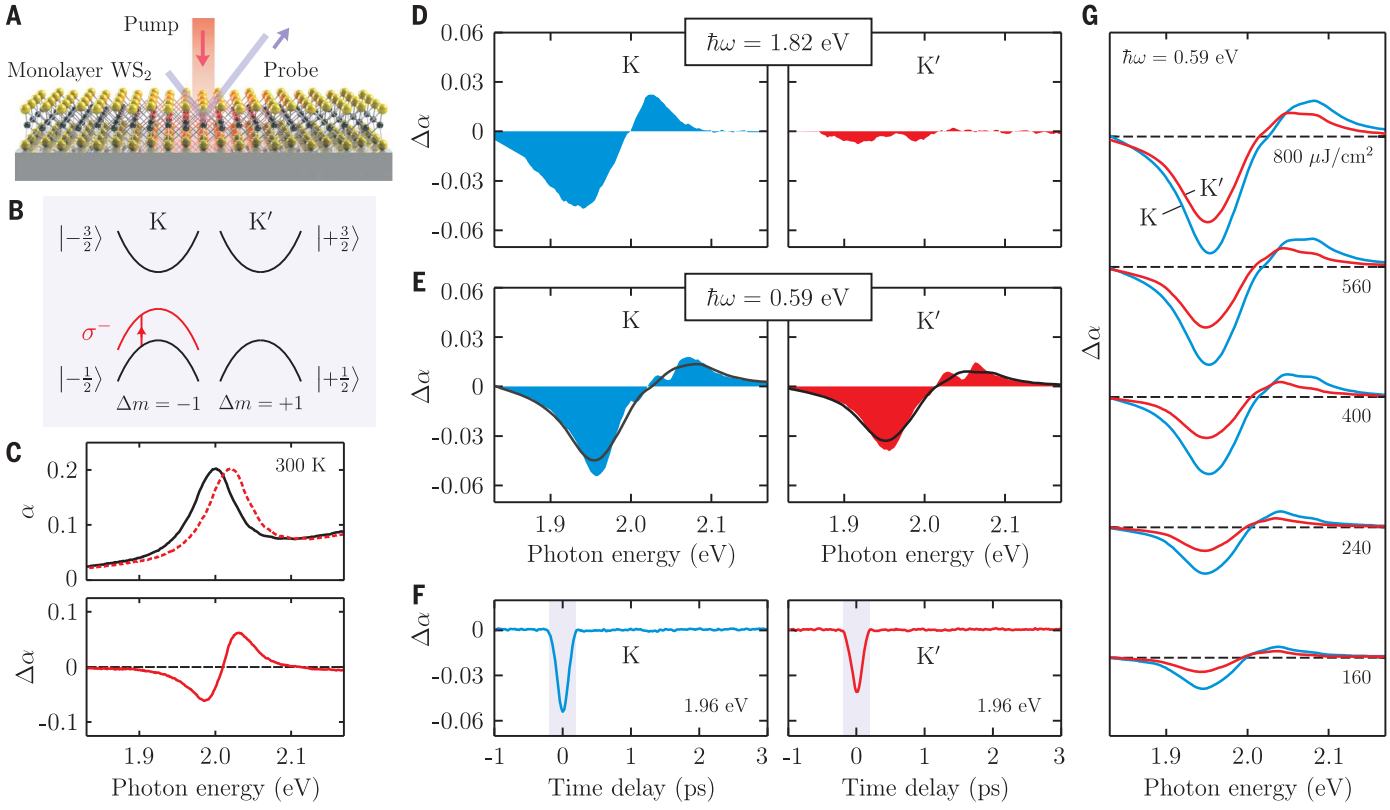

Fig. 2. Observation of valley-exclusive Bloch-Siegert shift in monolayer WS_2. (**A**) Illustration of the pump-probe experiment. We pump the monolayer WS_2 sample with strong infrared pulses and measure the pump-induced change of reflection with broadband probe pulses. (**B**) The *K* and *K′* valleys in monolayer WS_2. Optical pumping with left-handed circular polarization (σ^-) couples only to the *K* valley and not the *K′* valley, unless the counterrotating field is taken into account. (**C**) Top: Measured A exciton absorption spectrum (α, black curve) of monolayer WS_2 in equilibrium. The red dashed curve represents the shifted resonance (simulated) under red-detuned optical pumping. Bottom: This shift produces a differential curve in the absorption change ($\Delta\alpha$, red curve). (**D** and **E**) The $\Delta\alpha$ spectra under zero-delay optical pumping at pump photon energies of 1.82 and 0.59 eV. By using probe pulses with σ^- polarization, we can selectively measure $\Delta\alpha$ at the *K* valley; likewise, probe pulses with σ^+ polarization allow selective measurement of $\Delta\alpha$ at the *K′* valley (left and right panels, respectively). The black curves in (E) are smoothed curves to average out the modulations (see text). (**F**) Time trace of $\Delta\alpha$ spectra in (E) measured at probe energy of 1.96 eV and pump energy of 0.59 eV. The induced energy shift is observed only at zero time delay. (**G**) The zero-delay $\Delta\alpha$ spectra of the *K* valley (blue curves) and *K′* valley (red curves) under different incident pump fluences ($\mathcal{F}$ = 160 to 800 μJ/cm^2). The pump photon energy is 0.59 eV. The spectra are vertically displaced for clarity.

the *K* valley (*23*, *24*). The *K′* valley exhibits only a very weak (but observable) signal. However, as we lower the pumping photon energy to 0.59 eV, the signal at the *K′* valley becomes comparable to the signal at the *K* valley (Fig. 2E). This observation indicates a pronounced energy blueshift at the *K′* valley, a phenomenon that apparently violates the well-established valley selection rules in monolayer TMDs. Some modulations also appear in the $\Delta\alpha$ spectrum. These minor features are possibly induced by electron-phonon coupling and warrant further investigation; here, we average out these modulations by smoothing the curves (black lines). We further examined the signals at different pump-probe time delays. The $\Delta\alpha$ signals at both valleys emerge only at zero time delay, with temporal profiles very similar to the 160-fs duration of the pump pulses (Fig. 2F). These results indicate the coherent nature of the energy shift; they also exclude the influence of intervalley scattering of possible excited carriers, which typically occurs on the picosecond time scale (*25*–*27*).

To investigate the underlying mechanism of the anomalous energy shift at the *K′* valley, we measured the zero-delay $\Delta\alpha$ spectra for both valleys at various pump photon energies ($\hbar\omega$ = 0.59, 0.69, 0.89, or 0.98 eV) and different pump fluences ($\mathcal{F}$ = 30 to 800 μJ/cm^2). In Fig. 2G, we show the fluence-dependent spectra for $\hbar\omega$ = 0.59 eV (see fig. S1 for the remaining spectra). The $\Delta\alpha$ spectra at both valleys are found to grow with increasing pump fluence. For a more quantitative analysis, we extracted the energy shift from each spectrum, plotted as a function of $\mathcal{F}/(E_0 - \hbar\omega)$ in Fig. 3A. The shift at the *K* valley exhibits an excellent linear dependence regardless of the different pump photon energies (solid symbols), indicating that it arises from the optical Stark effect. The shift at the *K′* valley, however, spreads out with no rigorous linear dependence (open symbols). Such a contrast indicates that the *K′*-valley shift does not arise from the optical Stark effect. In Fig. 3B, we replot the *K′*-valley shift as a function of $\mathcal{F}/(E_0 + \hbar\omega)$ with the same axis scales; the data now exhibit an excellent linear dependence. Moreover, the slope of the *K′*-valley shift in this new plot is identical to the slope of the *K*-valley shift in Fig. 3A. This observation strongly suggests that the *K′*-valley shift arises from the Bloch-Siegert effect.

Our finding can be verified quantitatively by using either a semiclassical theory or a fully quantum-mechanical theory (*28*) (see supplementary text). Because we probe only the lowest-energy exciton state (1s), which shows properties similar to those of hydrogen atoms, it is appropriate and sufficient to use a simple two-level framework, as shown in earlier studies (*12*, *15*, *23*, *24*). In our semiclassical analysis, we treat the ground state and the 1s exciton state as a two-level system ($|a\rangle$ and $|b\rangle$) with a resonance energy E_0, driven by a classical electromagnetic wave with amplitude $\mathcal{E}_0$ and frequency ω. We use a left-circularly polarized pump beam,

$$\boldsymbol{\mathcal{E}}(t) = \mathcal{E}_0[\cos(kz - \omega t)\hat{x} + \sin(kz - \omega t)\hat{y}] \quad (1)$$

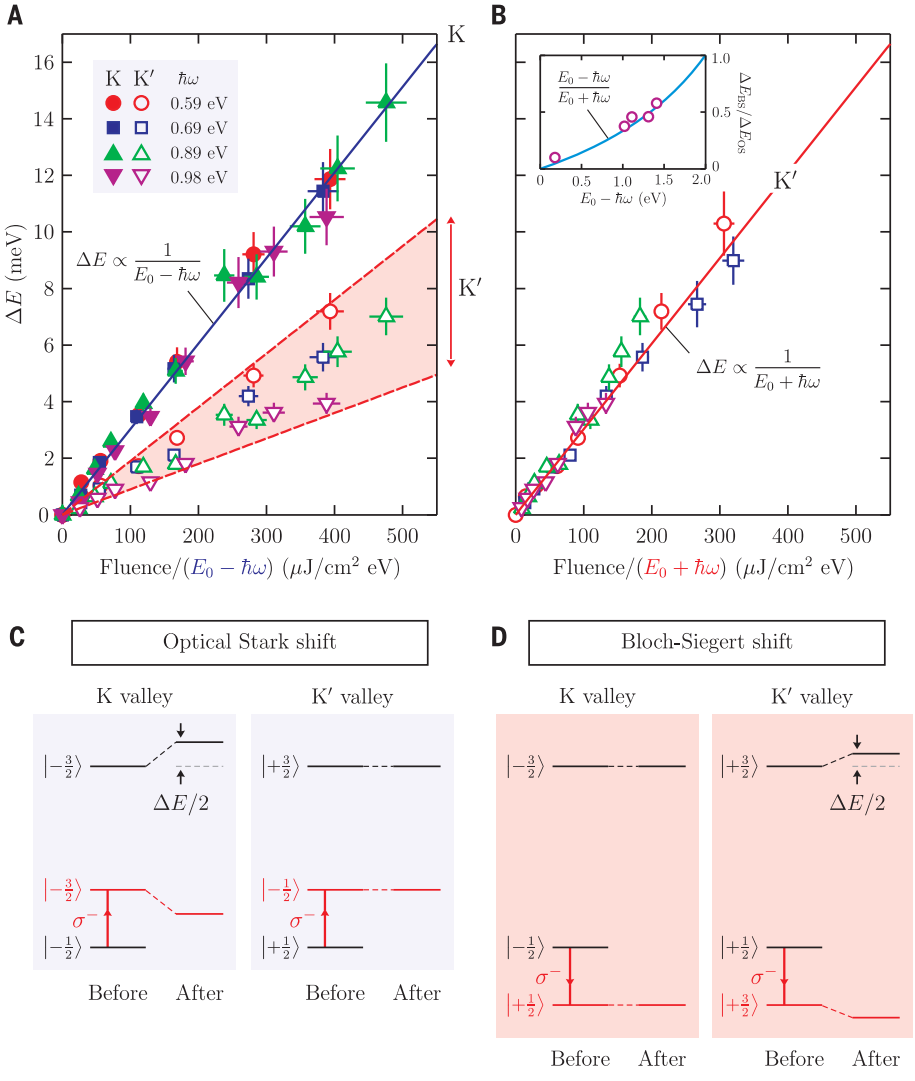

Fig. 3. Fluence and detuning dependences of the Bloch-Siegert shift. (**A**) Energy shifts at the *K* and *K*′ valleys (solid and open symbols) as a function of fluence $\mathcal{F}/(E_0 - \hbar\omega)$. The data are extracted from the $\Delta\alpha$ spectra in Fig. 2 and fig. S1. The *K*-valley shift exhibits a rigorous linear dependence (solid blue line), but the *K*′-valley shift spreads out (red region). (**B**) Energy shift at *K*′ valley as in (A), but plotted as a function of fluence $\mathcal{F}/(E_0 + \hbar\omega)$. The linear dependence becomes obvious. The inset at upper left shows the predicted ratio $\Delta E_{BS}/\Delta E_{OS}$ (blue line) when the detuning energy $(E_0 - \hbar\omega)$ increases from zero to the resonant energy (E_0 = 2 eV for monolayer WS_2). The open circles are our averaged experimental data obtained from Fig. 2 and fig. S1. (**C**) Energy diagram before and after optical pumping for the optical Stark shift, which occurs only at the *K* valley. (**D**) Energy diagram for the Bloch-Siegert shift, which occurs only at the *K*′ valley.

polarized along the *xy* plane of the monolayer sample (z = 0), which can also be expressed as

$$\boldsymbol{\mathcal{E}}(t) = \frac{1}{2}\mathcal{E}_0[(\hat{x} - i\hat{y})\exp(-i\omega t) + (\hat{x} + i\hat{y})\exp(i\omega t)] \quad (2)$$

where the field is decomposed into two terms according to their time-evolution factors $\exp(\pm i\omega t)$. The interaction Hamiltonian can then be expressed as

$$H_{ab} = \langle b|e\boldsymbol{\mathcal{E}}\cdot\mathbf{r}|a\rangle = \frac{1}{2}e\mathcal{E}_0\langle b|[(\mathbf{x} - i\mathbf{y})\exp(-i\omega t) + (\mathbf{x} + i\mathbf{y})\exp(-i\omega t)]|a\rangle \quad (3)$$

where the first term, $(\mathbf{x} - i\mathbf{y})\exp(-i\omega t)$, induces a transition with Δm = −1 (corotating field), and the second term, $(\mathbf{x} + i\mathbf{y})\exp(i\omega t)$, induces a transition with Δm = +1 (counterrotating field). Owing to the unique valley selection rules in monolayer WS_2, these two terms are thus coupled exclusively to the *K* (Δm = −1) and *K*′ (Δm = +1) valleys, respectively (Fig. 3, C and D), with their valley-specific interactions expressed as

$$H_{ab}(K) = \exp(-i\omega t)\frac{\mu_K\mathcal{E}_0}{2}$$
$$H_{ab}(K') = \exp(i\omega t)\frac{\mu_{K'}\mathcal{E}_0}{2} \quad (4)$$

Here, μ_K and $\mu_{K'}$ are the dipole matrix elements at the *K* and *K*′ valley, respectively, and they have equal magnitudes $\mu = |\mu_K| = |\mu_{K'}|$. However, they are associated with opposite time-evolution factors, which leads to a more general theory of valley selection rules in monolayer TMDs. Under the resonant absorption condition ($\hbar\omega = E_0$), the left-circularly polarized light couples only to the *K*-valley. By contrast, under the off-resonance condition ($\hbar\omega < E_0$), the coupling to the *K*′-valley can become appreciable through the time-reversed process, giving rise to a noticeable energy shift. The induced energy shifts at the respective valleys can be evaluated by the time-dependent perturbation theory as

$$\Delta E_K = \frac{\mu^2\mathcal{E}_0^2}{2}\frac{1}{E_0 - \hbar\omega}$$
$$\Delta E_{K'} = \frac{\mu^2\mathcal{E}_0^2}{2}\frac{1}{E_0 + \hbar\omega} \quad (5)$$

The two energy shifts have different energy dependence, from which we can readily identify ΔE_K to be the optical Stark shift and $\Delta E_{K'}$ the Bloch-Siegert shift. When plotted as a function of their respective energy denominators ($E_0 - \hbar\omega$ or $E_0 + \hbar\omega$), both shifts exhibit an identical slope. The prediction of common slope and opposite valley indices agrees well with our experimental observation (Fig. 3, A and B). From our data, we can deduce the dipole matrix elements to be μ = 55 debye, in excellent agreement with previous measurements (*23*). In addition, the ratio between $\Delta E_{K'}$ and ΔE_K is predicted to be $(E_0 - \hbar\omega)/(E_0 + \hbar\omega)$, the same as $\Delta E_{BS}/\Delta E_{OS}$ for a generic two-level system. By plotting the average shift ratio measured for each pump photon energy, we find good agreement between our experiment and theory (Fig. 3B, inset).

The physics of this valley-exclusive energy shift can be illustrated in the energy diagrams shown in Fig. 3, C and D. The corotating field generates a Floquet state $\hbar\omega$ above the ground state in both valleys, with energy separation $E_0 - \hbar\omega$ from the excited state. Because of the matching condition of angular momentum, repulsion between the Floquet state and the excited state only occurs at the *K* valley, giving rise to the ordinary optical Stark shift (Fig. 3C). On the other hand, the counterrotating field generates a Floquet state $\hbar\omega$ below the ground state, with energy separation $E_0 + \hbar\omega$ from the excited state (Fig. 3D). The matching condition of angular momentum forbids the level repulsion at the *K* valley but allows it at the *K*′ valley. This gives rise to the Bloch-Siegert shift at the opposite (*K*′) valley. In other words, the left-circularly polarized light can be understood as stimulating the σ^- absorption (Δm = −1) and σ^- emission (Δm = +1) processes at the *K* and *K*′ valleys, respectively. This makes it possible for the circularly polarized light with a given helicity to couple to both valleys in a distinct manner, thus enriching the valley selection rules.

The Bloch-Siegert shift we observed exhibits valley selection rules opposite from those of the

ordinary optical Stark effect, which allows us to completely separate the two effects. This is possible because, as time-reversed partners, the two effects share a similar relationship with the two time-reversed valleys in monolayer WS_2, which can be disentangled under circularly polarized light that breaks the time-reversal symmetry. Our finding reveals more general valley selection rules and may lead to enhanced control over the valleytronic properties of Dirac materials such as graphene, TMDs, and Weyl semimetals. Furthermore, by using higher pump intensity or lower pump photon energy with selective light helicity, we expect the emergence of higher-order coherent effects that could produce polarized valley current in transport experiments (*29*).

REFERENCES AND NOTES

1. C. Cohen-Tannoudji, J. Dupont-Roc, G. Grynberg, *Atom-Photon Interactions* (Wiley, 1998).
2. J. H. Shirley, *Phys. Rev.* **138**, B979–B987 (1965).
3. S. H. Autler, C. H. Townes, *Phys. Rev.* **100**, 703–722 (1955).
4. F. Bloch, A. Siegert, *Phys. Rev.* **57**, 522–527 (1940).
5. W. E. Lamb, R. C. Retherford, *Phys. Rev.* **72**, 241–243 (1947).
6. H. A. Bethe, *Phys. Rev.* **72**, 339–341 (1947).
7. R. Grimm, M. Weidemüller, Y. B. Ovchinnikov, *Adv. At. Mol. Opt. Phys.* **42**, 95–170 (2000).
8. P. Forn-Díaz *et al*., *Phys. Rev. Lett.* **105**, 237001 (2010).
9. J. Tuorila *et al*., *Phys. Rev. Lett.* **105**, 257003 (2010).
10. T. Niemczyk *et al*., *Nat. Phys.* **6**, 772–776 (2010).
11. K. F. Mak, C. Lee, J. Hone, J. Shan, T. F. Heinz, *Phys. Rev. Lett.* **105**, 136805 (2010).
12. A. Chernikov *et al*., *Phys. Rev. Lett.* **113**, 076802 (2014).
13. X. Liu *et al*., *Nat. Photonics* **9**, 30–34 (2014).
14. D. Xiao, G.-B. Liu, W. Feng, X. Xu, W. Yao, *Phys. Rev. Lett.* **108**, 196802 (2012).
15. K. F. Mak, K. He, J. Shan, T. F. Heinz, *Nat. Nanotechnol.* **7**, 494–498 (2012).
16. H. Zeng, J. Dai, W. Yao, D. Xiao, X. Cui, *Nat. Nanotechnol.* **7**, 490–493 (2012).
17. T. Cao *et al*., *Nat. Commun.* **3**, 887 (2012).
18. S. Wu *et al*., *Nat. Phys.* **9**, 149–153 (2013).
19. X. Xu, W. Yao, D. Xiao, T. F. Heinz, *Nat. Phys.* **10**, 343–350 (2014).
20. K. F. Mak, K. L. McGill, J. Park, P. L. McEuen, *Science* **344**, 1489–1492 (2014).
21. P. Rivera *et al*., *Science* **351**, 688–691 (2016).
22. J. R. Schaibley *et al*., *Nat. Rev. Mater.* **1**, 16055 (2016).
23. E. J. Sie *et al*., *Nat. Mater.* **14**, 290–294 (2015).
24. J. Kim *et al*., *Science* **346**, 1205–1208 (2014).
25. C. Mai *et al*., *Nano Lett.* **14**, 202–206 (2014).
26. C. Mai *et al*., *Phys. Rev. B* **90**, 041414(R) (2014).
27. E. J. Sie, A. J. Frenzel, Y.-H. Lee, J. Kong, N. Gedik, *Phys. Rev. B* **92**, 125417 (2015).
28. M. D. Crisp, *Phys. Rev. A* **43**, 2430–2435 (1991).
29. A. Kundu, H. A. Fertig, B. Seradjeh, *Phys. Rev. Lett.* **116**, 016802 (2016).

ACKNOWLEDGMENTS

We thank Q. Ma and Y. Bie for the assistance during absorption measurement. N.G. and E.J.S. thank M. Zwierlein and J. Kono for the stimulating discussions. N.G. and E.J.S. acknowledge support from the U.S. Department of Energy, BES DMSE (experimental setup and data acquisition), and from the Gordon and Betty Moore Foundation's EPiQS Initiative grant GBMF4540 (data analysis and manuscript writing); J.K. and L.F. acknowledge support from NSF Science and Technology Center for Integrated Quantum Materials grant DMR-1231319 (material growth and theory); Y.-H.L. acknowledges support from the Asian Office of Aerospace Research and Development/Office of Naval Research Global grant FA2386-16-1-4009 and Ministry of Science and Technology, Taiwan, grants 105-2112-M-007-032-MY3 and 105-2119-M-007-027 (material growth).

SUPPLEMENTARY MATERIALS

www.sciencemag.org/content/355/6329/1066/suppl/DC1
Materials and Methods
Supplementary Text
Figs. S1 to S4
References (*30*–*34*)

15 October 2016; accepted 8 February 2017
10.1126/science.aal2241

Large, valley-exclusive Bloch-Siegert shift in monolayer WS_2
Edbert J. Sie, Chun Hung Lui, Yi-Hsien Lee, Liang Fu, Jing Kong and Nuh Gedik (March 9, 2017)
Science **355** (6329), 1066-1069. [doi: 10.1126/science.aal2241]

Editor's Summary

Going way off resonance

Single atomic layers of transition metal dichalcogenide (TMD) materials have two nonequivalent valleys in their electronic structure. When researchers shine visible light on these monolayers, left-circularly polarized light modifies the electronic levels in one valley but not the other. Sie *et al.* studied the material WS_2. They found that in the infrared regime, if the frequency of the light was far away from the resonance, energy levels in both valleys were affected. The so-called Bloch-Siegert effect could explain the energy shift in the "wrong" valley. The findings should be important for the manipulation of valleytronic properties of TMDs.

Science, this issue p. 1066